Journées du Groupe de Travail en Modélisation Géométrique, Palaiseau, 2021

Measuring Holes of 3D Meshes

Yann-Situ Gazull[1], Aldo Gonzalez-Lorenzo[1] and Alexandra Bac[1]

[1]Université d'Aix-Marseille

Abstract

In algebraic topology, persistent homology is a method that computes the homology of an object growing in time. Intuitively, this technique detects holes and provides information on their importance. By combining this topological approach to a notion of distance, it is possible to obtain geometric information on those holes. This paper presents an ongoing work about computation and measure of holes in 3D volumetric objects. Our approach uses mainly the geometric and topological properties of the medial axis.

Keywords: Geometric Modeling, Algebraic Topology, Medial Axis, Persistent Homology.

1. Introduction

In this paper, we introduce a new ongoing work about measuring holes in 3D shapes. Paradoxically, holes are intuitive objects that are topologically quite complex to define. However their topological definition doesn't take into account their geometrical properties. We propose ideas about how to geometrically measure the topological holes of a 3D object. Our approach uses the medial axis. It is a geometric notion that preserves topological features, that is why it is suited to our problem. More precisely, we believe that the computation of the medial axis gives enough information to associate two independent measures to holes. One measure stands for the *thickness* whereas the other stands for the *breadth* of the hole.

Concerning applications, hole measures provides a relevant object descriptor, as highlighted in [CCSG*09], that can be useful for classification. They can also have biological applications, such as pollen characterization and porosity estimation.

Our approach uses persistent homology, which is a method that computes the homology of an object growing in time. Instead of performing persistent homology algorithms on the analyzed object (which requires a precise and expensive tetrahedralization), we show that performing these algorithms on the medial axis is sufficient to obtain the thickness and breadth of the holes of the object.

The structure of the paper is as follows. In section 2 we introduce previous works on hole measures and our two main tools: persistent homology and medial axes. Our approach is explained in section 3: we first give an overview with notations and we then detail the two parts of our method. The second part mostly consists in conjectures. In section 4 we present algorithmic prospects for our approach, more specifically we describe methods for computing the medial axis. Conclusion is provided in section 5.

2. Related Works

2.1. Persistent Homology

Given a topological set X, let $H_q(X)$ be the homology group of dimension q over the field $\mathbb{Z}_2$. Every $H_q(X)$ is a vector space of dimension β_q, where β_q is called the q-th Betti number. Intuitively, the Betti numbers are counting the *holes* in X: in 3D, β_0 is the number of connected components, β_1 is the number of tunnels and β_2 is the number of cavities in X. See [Hat] for more details on homology and more generally algebraic topology.

Persistent homology is a recent theory, closely related to Morse theory. It somehow "equips" topological artifacts with a notion of "size" by following their appearance and disappearance through the growth of a discrete object along time. More precisely, persistent homology captures the changes in homology along a filtration of a topological set X.

Definition 2.1. A filtration of X is a sequence $(F_t)_{t\in I}$ of

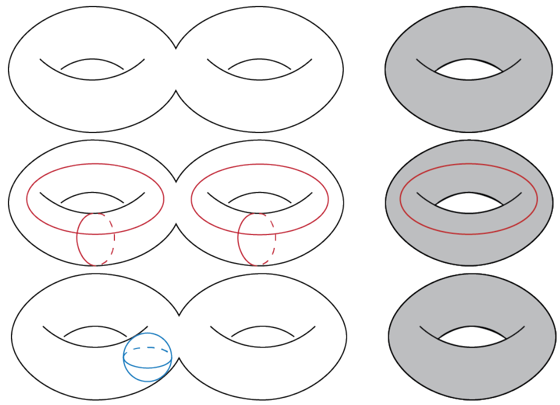

Figure 1: Each row is the same object: a hollow two-tore with a plain tore (in grey). It has 2 connected components, 5 tunnels (in red) and a single cavity (in blue). Its Betti numbers are: $\beta_0 = 2$, $\beta_1 = 5$ and $\beta_2 = 1$.

subsets of X verifying :

$$t \le t' \implies F_t \subset F_{t'}$$
$$F_{\sup(I)} = X$$

Where I can be a real interval or a finite ordered set.

Persistence keeps track of the birth and death of holes along the filtration. This information is summed up trough a *persistence diagram*:

Definition 2.2. The persistence diagram $\mathcal{D}(F)$ of a filtration F is a multi set of $\mathbb{R}^2$. An element (x,y) of multiplicity $\beta_q^{x,y}$ means that $\beta_q^{x,y}$ holes of dimension q were born in F_x and died entering F_y.

Therefore $y-x$ is the “lifetime” of the corresponding hole and significant holes are points of $\mathcal{D}(F)$ lying far from the diagonal $y = x$.

In practice, X is a finite discrete complex and the filtration consists in labeling every cell with their date of birth. The standard algorithm to compute the persistence diagram of a filtration on a simplicial complex X uses matrix operations on the boundary operator [OPT*15, EH08]. It has a complexity in $\mathcal{O}(n^3)$ where n is the number of simplices in X.

2.2. Hole Measures

Persistent homology can provide geometrical information on topological artifacts if the filtration has a geometrical meaning. An example of such a filtration is induced by the *signed distance function*:

Definition 2.3. Given a set X in $\mathbb{R}^n$, the *signed distance function* of X is the following function:

$$\begin{aligned} sdf : \mathbb{R}^n &\to \quad \mathbb{R} \\ x &\mapsto -d(x,\partial X) \qquad \text{if } x \in X \\ x &\mapsto \ \ d(x,\partial X) \qquad \text{if } x \notin X \end{aligned}$$

Where d is the euclidean distance in $\mathbb{R}^n$.

Proposition 2.1. *The sequence* $\left(sdf^{-1}(]-\infty,t[)\right)_{t\in\mathbb{R}}$ *is a filtration. We refer to it as the sdf-filtration.*

Starting from the persistence of this filtration, Gonzalez-Lorenzo and al. define geometric measures of topological holes (in [GLBMR16]). Indeed, if we consider a hole that was born at time $x \le 0$ and dies at time $y \ge 0$ (a point (x,y) in the up-left quarter of the diagram) we can define the *thickness* T and the *breadth* B of the hole as follow:

$$T = -x \qquad\qquad B = y$$

Intuitively, the thickness of the hole corresponds to the fragility of the hole handles. The breadth, on the other side, corresponds to the size of the hole. Those measures can be associated with balls: the T-ball (respectively the B-ball) is the ball of radius T (respectively B) whose center is the point that induced the birth of the hole at time $-T$ (respectively the point that induced the death of the hole at time $+B$) (see Figure 2(b)). Points that induce birth or death of a hole are called *topologically critical points* and play a key role in our work.

In [GLBMR16], these measures (called *TB-measures*) are introduced and computed for cubical complexes. However their definition takes advantage of the structure of cubical complexes: the regularity of voxels actually captures an information of geometric nature right into the topological notion of adjacency. As a consequence, in this context, the "distance to the center of the shape" is naturally captured by the signed distance transform, ie. by dilatation/erosion operations. In simplicial complexes, this is no longer the case and our present work intends to extend holes measures to this wider context.

2.3. Medial Axis

The medial axis of a set X is a geometric object that has a large number of characterizations [TDS*16]. In this paper we will take the following definition:

Definition 2.4. If X is embedded in $\mathbb{R}^n$, the *medial axis* $\mathcal{M}(X)$ of X is the set of points in $\mathbb{R}^n$ that have two or more closest points on ∂X (the boundary of X).

We refer to the *inner medial axis* as

$$\check{\mathcal{M}}(X) = \mathcal{M}(X) \cap X$$

and to the *outer medial axis* as

$$\hat{\mathcal{M}}(X) = \mathcal{M}(X) \cap (\mathbb{R}^n \backslash X) = \check{\mathcal{M}}(\mathbb{R}^n \backslash X)$$

(see an illustration of the medial axis in Figure 2(a))

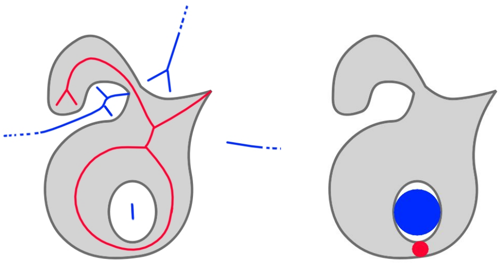

(a) (b)

Figure 2: (a): X in grey with its medial axis: $\check{\mathcal{M}}(X)$ in red and $\hat{\mathcal{M}}(X)$ in blue.
(b): the T-ball (in red) and the B-ball (in blue) of the only 1-hole in X.

The medial axis is widely used for different purposes such as skeleton creation or reconstruction problems [TDS*16]. Concerning topology, it is known that $\check{\mathcal{M}}(X)$ preserves homotopy :

Proposition 2.2 ([Lie03]). *For all bounded open X:*

$$\check{\mathcal{M}}(X) \approx X \tag{1}$$

Where $\approx$ stands for homotopy equivalence.

The combination of geometrical and topological properties has made it a powerful tool and has lead to several works at the intersection of those two fields. For example Zhou et al [ZJH07] developed a method to repair the topology of some 3D shapes.

3. Measuring Holes of 3D Volumetric Objects

3.1. Overview of the Approach

The aim of our work is to find a method to compute hole measures (i.e. TB-balls) on 3D meshes. More precisely we are dealing with 3D compact volumes, the boundary of which is an oriented mesh (2-manifold). In this section, our theoretical work is more general, so we will be using $\mathbb{R}^n$ instead of $\mathbb{R}^3$.

The persistence homology of the sdf-filtration provides different holes, which can be classified in two non-disjoint categories:

- *Early-birth holes*, whose birth date is before 0 (called an *early-birth date*).
- *Late-death holes*, whose death date is after 0 (called a *late-death date*).

Remark. We also use the terms *late-birth* for birth date after 0, and *early-death* for death date before 0.

The holes we are interested in are those in the object at $t = 0$, i.e. those in the intersection of the early-birth holes and the late-death holes. We refer to them as the TB-*holes*, as they are the holes associated with the TB-balls: T is the opposite of the early-birth date and B is the late-death date.

Our approach intends to compute the TB-balls and relies on two main points, detailed in sections 3.3 and 3.4:

1. Considering a bounded open $X \subset \mathbb{R}^n$, we show that the persistent homology of its inner medial axis using the sdf-filtration provides every early-birth and early-death date with their associated topologically critical points. Particularly, it provides the T-balls of X.
2. We believe that the same technique on the outer medial axis with the opposite filtration provides every early-birth and early-death date of the complementary of X in the n-sphere, with their critical points.
   Relying on Alexander duality, we think it is then possible to deduce every late-death and late-birth date of X with their critical points. Particularly, we can deduce the B-balls of X.

All in all, the persistent homology of each part of the medial axis should provide the TB-balls.

3.2. Preliminaries and Notations

Theoretically, our goal is to obtain the persistence diagram of the sdf-filtration and the topologically critical points associated to each hole.

Definition 3.1. Given an open bounded set $X \subseteq \mathbb{R}^n$ and its signed distance function sdf, we define the sdf filtration function:

$$\begin{array}{rrcl} \mathcal{F}_t: & \mathcal{P}(\mathbb{R}^n) & \to & \mathcal{P}(\mathbb{R}^n) \\ & U & \mapsto & sdf^{-1}(]-\infty,t[) \cap U \end{array}$$

(see an illustration in Figure 3) In particular, if $t \geq 0$, we have $\mathcal{F}_{-t}(U) \subset X$ for all $U \subset \mathbb{R}^n$ and $\mathcal{F}_{-t}(V) = sdf^{-1}(]-\infty,-t[)$ for all $V \supset X$.

The filtration we are interested in is the sdf-filtration, which is equal to $\left(\mathcal{F}_t(\mathbb{R}^n)\right)_{t\in\mathbb{R}}$.

In section 3.4 we will establish conjectures on the complementary of X in the n-sphere S^n. Precisely, we are mapping $\mathbb{R}^n$ to S^n by identifying all the points that are located at infinity in $\mathbb{R}^n$ to a single point p_∞. Particularly we can consider that we have $\mathbb{R}^n \subset S^n$.

Definition 3.2. Given X a bounded open in $\mathbb{R}^n$, the complementary of X in S^n is:

$$X^c = S^n \backslash X$$

We denote sdf^c its signed distance function in S^n which is equal $-\infty$ on p_∞ and $-sdf$ elsewhere.

Definition 3.3. We denote $\mathcal{F}^c_t$ the sdf filtration function of X^c in S^n:

$$\begin{array}{rrcl} \mathcal{F}^c_t: & \mathcal{P}(S^n) & \to & \mathcal{P}(S^n) \\ & U & \mapsto & (sdf^c)^{-1}([-\infty,t]) \cap U \end{array}$$

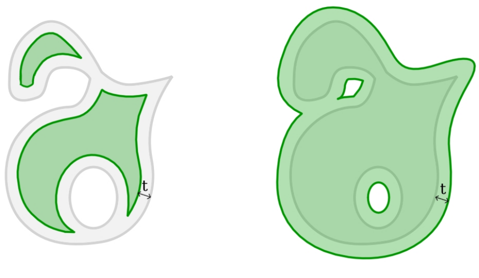

(a) (b)

Figure 3: t is a positive real.
(a): the t-erosion of X (in green). Formally, it is $\mathcal{F}_{-t}(\mathbb{R}^n)$, which is equal to $\mathcal{F}_{-t}(X)$ or simply $sdf^{-1}(]-\infty,-t[)$. We can see that the erosion creates a new component but delete a 1-hole.
(b): the t-dilatation of X (in green). Formally, it is $\mathcal{F}_t(\mathbb{R}^n)$. We can see that the dilatation creates a new 1-hole.

We refer to $(\mathcal{F}^c_t(S^n))_{t\in\mathbb{R}}$ as the sdf^c-filtration.

Intuitively, erosion in the sdf-filtration correspond to dilatation in the sdf^c-filtration and vice-versa.

Definition 3.4. We denote $\mathcal{M}_{S^n}(X)$ the medial axis of X computed on S^n but with the metric distance of $\mathbb{R}^n$.
It can be noted that $\mathcal{M}_{S^n}(X)$ is equal to $\mathcal{M}(X) \cup \{p_\infty\}$ and p_∞ belongs to X^c. (See an illustration of $\mathcal{M}_{S^n}(X)$ in Figure 5)

3.3. Obtaining T-Balls from the Inner Medial Axis

The medial axis has been a subject of interest since it is a geometrical object that has a powerful topological property (see Proposition 1). In this part, a deeper link between the topology and the geometry of $\check{\mathcal{M}}(X)$ and X is introduced: the persistence diagram of the sdf-filtration on $]-\infty,0]$ is the same as the one obtained with the sdf-filtration restricted to $\check{\mathcal{M}}(X)$.
This result is stated in theorem 3.3. It implies that computing the persistent homology of $\check{\mathcal{M}}(X)$ on $]-\infty,0]$ provides early-birth and early-death dates with their associated topologically critical points and therefore the T-balls of X.

To prove this result we first need to prove the following theorem:
Theorem 3.1. *Given X an open bounded set of $\mathbb{R}^n$ and $t \geq 0$:*

$$\mathcal{F}_{-t}\Big(\check{\mathcal{M}}(X)\Big) = \check{\mathcal{M}}\Big(\mathcal{F}_{-t}(X)\Big)$$

An illustration of the theorem is showed in Figure 4.

The proof is geometrical and can be found in the appendix 5.
This implies the following property:

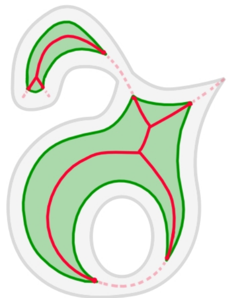

Figure 4: An illustration of theorem 3.1. The red curve is the medial axis of the green shape: $\check{\mathcal{M}}(\mathcal{F}_{-t}(X))$. It is also the intersection between the medial axis of X (the dashed curve) and the green shape: $\mathcal{F}_{-t}\left(\check{\mathcal{M}}(X)\right)$.

Corollary 3.2. *Given X an open bounded set of $\mathbb{R}^n$ and $t \geq 0$:*

$$\mathcal{F}_{-t}\Big(\check{\mathcal{M}}(X)\Big) \approx \mathcal{F}_{-t}(X)$$

Proof. As $t \geq 0$, $sdf^{-1}(]-\infty,-t[) \subset X$ so we have $\mathcal{F}_{-t}(X) = sdf^{-1}(]-\infty,-t[)$.
Hence, $\mathcal{F}_{-t}(X)$ is open because sdf is continuous and $]-\infty,t[$ is open. Moreover it is bounded because it is contained in X.
Using equation 1 on $\mathcal{F}_{-t}(X)$ we obtain:

$$\check{\mathcal{M}}(\mathcal{F}_{-t}(X)) \approx \mathcal{F}_{-t}(X)$$

Combined to theorem 3.1 we get the wanted result. □

Theorem 3.3. *Given X an open bounded set of $\mathbb{R}^n$ and its associated functions $\mathcal{F}_t$:*

$$\mathcal{D}\left(\left(\mathcal{F}_t(\mathbb{R}^n)\right)_{t\in]-\infty,0]}\right) = \mathcal{D}\left(\left(\mathcal{F}_t(\check{\mathcal{M}}(X))\right)_{t\in]-\infty,0]}\right)$$

Proof. At every step $t \in]-\infty,0]$ of the filtration we have $\mathcal{F}_t(\mathbb{R}^n) = \mathcal{F}_t(X)$. By corollary 3.2, $\mathcal{F}_t(\mathbb{R}^n)$ and $\mathcal{F}_{-t}\left(\check{\mathcal{M}}(X)\right)$ have the same homotopy type. Therefore, they have isomorphic homology groups (see theorem 2.10 in [Hat] (p.111)).
Hence, their persistent homology and persistence diagrams are similar. □

As a consequence the persistence diagram of X on $]-\infty,0]$ can be obtained by performing the persistence algorithm on its inner medial axis. As we are on $]-\infty,0]$, this diagram gives every early-birth and early-death date, but we also need the ball centers in order to fully obtain the T-balls. Fortunately we have the following proposition, which can be deduced from results in [CPP08] and [Sie96]:

Proposition 3.4. *The topologically critical points of* $(\mathcal{F}_t(\mathbb{R}^n))_{t\in]-\infty,0]}$ *are exactly the topologically critical points of* $\left(\mathcal{F}_t(\check{\mathcal{M}}(X))\right)_{t\in]-\infty,0]}$.

As the standard persistence algorithm also computes the topologically critical points, performing the persistence algorithm on $\check{\mathcal{M}}(X)$ fully provides the T-balls.

3.4. Obtaining B-balls using the Outer Medial Axis and Alexander Duality

This part is an ongoing work in which we establish conjectures. We aim to capture the persistence on $[0,+\infty[$ (i.e. the B-balls, late-death and late-birth dates) using the outer medial axis of X and the *Alexander duality*, which provides topological links between X and its complementary.

Proposition 3.5 (Alexander Duality, [Hat], (p.255))**.** *If K is a locally contractible nonempty compact of S^n, then:*

$$\forall i, \quad \tilde{H}_i(S^n \backslash K) \simeq \tilde{H}^{n-i-1}(K)$$

Where $\tilde{H}_j$ and $\tilde{H}^j$ are the reduced homology and cohomology groups, and $\simeq$ stands for isomorphism.

This implies that we can obtain the Betti numbers of K from those of its complement in S^n. For instance, in 3D:

$$\beta_0(K) = \beta_2(S^3\backslash K)+1$$
$$\beta_1(K) = \beta_1(S^3\backslash K)$$
$$\beta_2(K) = \beta_0(S^3\backslash K)-1$$

(See an illustration of Alexander duality in Figure 5)

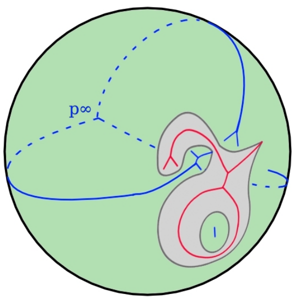

Figure 5: An illustration of Alexander duality and the medial axis $\mathcal{M}_{S^2}(X)$. In 2D, Alexander duality implies $\beta_0(X) = \beta_1(X^c)+1$ and $\beta_1(X) = \beta_0(X^c)-1$:
X (in grey) has one component and one 1-hole.
X^c (in green) has two components and no 1-hole.
In red: $\check{\mathcal{M}}_{S^2}(X)$. In blue: $\hat{\mathcal{M}}_{S^2}(X)$ which equals to $\check{\mathcal{M}}_{S^2}(X^c)$.

Similarly to section 3.3, we think the following link between the topology and the geometry of X and its outer medial axis $\check{\mathcal{M}}_{S^n}(X^c)$ is true: the persistence diagram of the *sdf*-filtration on $[0,+\infty[$ can be deduced from the diagram of the sdf^c-filtration restricted to $\check{\mathcal{M}}_{S^n}(X^c)$.

This result is stated in conjecture 3.9. It implies that computing the persistent homology on $\check{\mathcal{M}}_{S^n}(X^c)$ provides late-death and late-birth dates of X.

Our idea is to prove this result using the same reasoning as the one in section 3.3 leading to theorem 3.3.
To do so we need to prove the three following conjectures, which corresponds to "Alexander duals" of theorems in section 3.3. We believe they are true under reasonable assumptions on X, such as the fact that X is a bounded open and $X \cup \partial X$ has the same homotopy type as X.

Conjecture 3.6 (dual of theorem 3.1)**.** *Given $t \geq 0$:*

$$\mathcal{F}^c_{-t}\left(\check{\mathcal{M}}_{S^n}(X^c)\right) = \check{\mathcal{M}}_{S^n}\left(\mathcal{F}^c_{-t}(X^c)\right)$$

Conjecture 3.7 (dual of corollary 3.2)**.** *Given $t \geq 0$:*

$$\mathcal{F}^c_{-t}\left(\check{\mathcal{M}}_{S^n}(X^c)\right) \approx \mathcal{F}^c_{-t}(X^c)$$

Conjecture 3.8 (dual of theorem 3.3)**.**

$$\mathcal{D}\left((\mathcal{F}^c_t(S^n))_{t\in]-\infty,0]}\right) = \mathcal{D}\left((\mathcal{F}^c_t(\check{\mathcal{M}}_{S^n}(X^c)))_{t\in]-\infty,0]}\right)$$

Conjecture 3.8 implies that the persistence diagram of $\check{\mathcal{M}}_{S^n}(X^c)$ with the sdf^c-filtration gives every early-birth and early-death date of X^c.
Relying on Alexander duality, we believe that these information provides every late-death and late-birth date of X, according to the following transformation:
Conjecture 3.9.

$$\mathcal{D}\left((\mathcal{F}_t(R^n))_{t\in[0,+\infty[}\right) = \tilde{\mathcal{D}}\left((\mathcal{F}^c_t(\check{\mathcal{M}}_{S^n}(X^c)))_{t\in]-\infty,0]}\right)$$

Where $\tilde{\mathcal{D}}$ stands for a deduction from the underlying diagram following Alexander duality: the i-holes of coordinates (x,y) becomes $(n-i-1)$-holes of coordinates $(-y,-x)$, except for the oldest 0-hole which has no dual. A 0-hole whose death date is infinite and birth date is before 0 is also added.

The main idea of the proof would be that at each step $\tau \geq 0$ we have $\mathcal{F}^c_{-\tau}(S^n) = S^n \backslash \mathcal{F}_\tau(R^n)$ (using the definitions of $\mathcal{F}^c_{-\tau}$ and $\mathcal{F}_\tau$). By Alexander duality, this means that when a i-hole appears in $(\mathcal{F}^c_t(S^n))_{t\in]-\infty,0]}$ at step $-\tau$, a $(n-i-1)$-hole disappears in $(\mathcal{F}_t(R^n))_{t\in[0,+\infty[}$ at step τ, and vice-versa.

To fully find the B-balls of X, we also need the dual of proposition 3.4:
Conjecture 3.10 (dual of proposition 3.4)**.** *The topologically critical points of $(\mathcal{F}_t(\mathbb{R}^n))_{t\in[0,+\infty[}$ are exactly the topologically critical points of $\left(\mathcal{F}^c_t(\check{\mathcal{M}}_{S^n}(X^c))\right)_{t\in]-\infty,0]}$, but appears in the inverse order.*

Hence, the persistence diagram of the outer medial axis $\check{\mathcal{M}}_{S^n}(X^c)$ with the sdf^c-filtration induces the deduction of every late-death and late-birth date of X with their critical points. Therefore, it fully provides the B-balls.

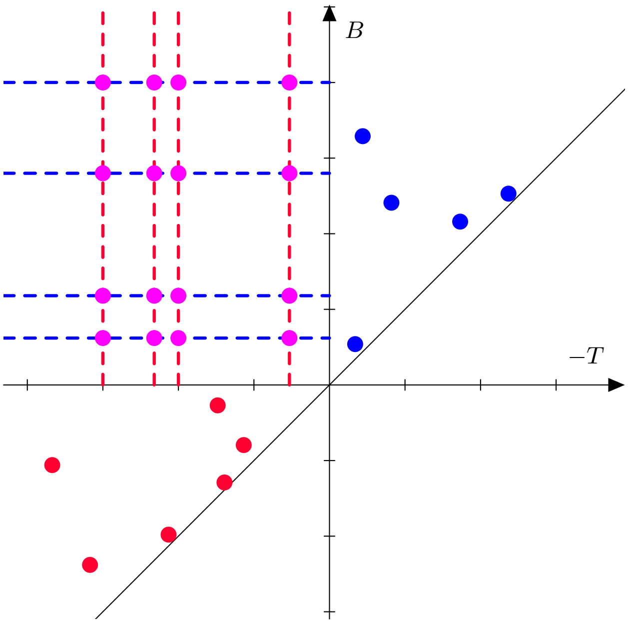

Figure 6: A partial persistence diagram. The red elements (dots and semi-lines) are early-birth and early-death dates obtained from persistence on $\check{\mathcal{M}}(X)$ (see section 3.3) whereas those in blue are late-death and late-birth dates obtained by Alexander duality from persistence on $\hat{\mathcal{M}}_{S^n}(X)$ (see section 3.4).
The magenta dots are the potential holes, obtained from matching the red lone T values with the blue lone B values. There are actually four unknown dots and they cannot be two on the same line or on the same column.

All in all, computing the persistence of the inner and outer medial axes of X (using their appropriate filtration) gives enough information to obtain every TB-ball of X. However, a subtle topological information is missing: we are not able to decide which T corresponds to which B, therefore we only get a partial persistence diagram of X (see an illustration on Figure 6).

4. Algorithmic prospects

Our method can be summed up in the following algorithm:

1. Compute the inner and outer medial axis of X.
2. Perform persistence algorithm on the inner medial axis with the sdf-filtration on $]-\infty,0]$ and retain its topologically critical points.
3. Perform persistence algorithm on the outer medial axis with the sdf^c-filtration on $]-\infty,0]$ and retain its topologically critical points.
4. Using Alexander duality, deduce from the two last results the partial persistence diagram of X with its TB-balls.

In practice, we first need to compute a discrete representation of the medial axis and label its elements with their sdf value. In addition we want this representation to provide topologically critical points of X.
Different methods computing such a representation have been created:
Sundar et al [SMM20] proposed a geometrical method for computing the medial axis with its critical points using touching discs. However their approach works in 2D and can hardly be generalized to 3D. Culver et al [CKM04] proposed an algorithm that exactly computes the medial axis of a polyhedron, but it is highly expensive in time.

Dey et al [DZ04] proposed a method, based on Voronoi diagrams of point sampling, that approximates the medial axis. Although their approach is quite fast, their approximation lacks topological guarantees. But even if the representation of the medial axis is not exact, we think that the stability of persistent homology should limit the errors in our method (see [CSEH05] for details about stability). Finally, Giensen et al [GRB11] proposed another method based on Voronoi diagrams that provides topological guarantees and critical points. Instead of computing $\mathcal{M}(X)$, their method computes *the core of* X, which is a subset of the medial axis having the following desired properties: it contains the critical points of the medial axis (so the one of X) and it has the same homotopy type as X. Yet, this algorithm requires an ϵ-sampling of the boundary of X with $\epsilon \leq 0.14$ to ensure homotopy:

Definition 4.1 ([GRB11]). An ϵ-sampling of the surface ∂X of X is a set $P \subset \partial X$ such that:

$$\forall x \in \partial X,\ \exists p \in P\ / \quad d(x,p) \leq \epsilon\, d(x, \check{\mathcal{M}}(X))$$

(see an illustration in Figure 7(b))

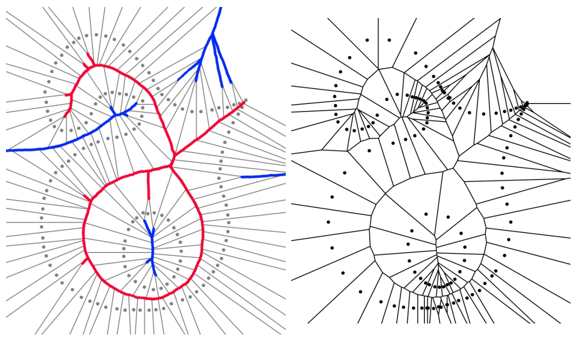

(a) (b)

Figure 7: (a): An approximation of the medial axis, as a subcomplex of the Voronoi diagram of a sampling of ∂X.
(b): An ϵ-sampling of ∂X and its associated Voronoi diagram. We see that this sampling is adaptive to the local thickness of the shape.

The two last approaches are promising and use Voronoi diagrams, which are often considered as discrete medial axes (in fact they corresponds to medial axes of discrete sets of points) (see Figure 7 for approximations using Voronoi diagrams). An advantage of these approaches is the computation of topologically critical points because their discrete counterparts are simply the intersections of Voronoi cells with their dual Delaunay cells [GRB11]. However, both approaches need a sampling of the boundary of X, which can be challenging to build.

5. Conclusion and Future Works

We are currently developing a new method to compute measures of holes in 3D volumetric shapes. Our algorithm is based on the theory of persistent homology and uses the notion of medial axis, which provides a powerful link between geometry and topology. Our method pretends to compute every TB-ball of the analyzed shape.

An advantage of the approach is that we compute persistent homology on the medial axis which has one dimension less than the object, for instance if X is a volumetric 3D object, $\mathcal{M}(X)$ is set of curves and surfaces. However, the medial axis computation in 3D is far from free, and we are interested in specific part of it. That is why it will be crucial to find an appropriate method for its computation in order to finally implement our approach. *Voronoi subset* and *distance flow* approaches [DZ04, GRB11, CPP08] seem suited for our problem.

Although our approach provides every TB-ball, strangely enough, medial axis persistence (and Alexander duality) seem not to pair lone T and B-balls. Hence, they would not provide a complete persistence diagram. Actually, this information might have a geometrical nature (this difference between topology and geometry may be occluded in cubical complexes). However, we assume that the geometry of medial axes with respect to X actually provides this connection information. Therefore, an idea is to build a filtration on a simplicial complex derived from a Voronoi approximation of the medial axis (as in Figure 7(a)).

References

[CCSG*09] CHAZAL F., COHEN-STEINER D., GUIBAS L., MÉMOLI F., OUDOT S.: Gromov-hausdorff stable signatures for shapes using persistence. *Comput. Graph. Forum. Vol. 28* (07 2009), 1393–1403.

[CKM04] CULVER T., KEYSER J., MANOCHA D.: Exact computation of the medial axis of a polyhedron. *Comput. Aided Geom. Des.. Vol. 21*, Num. 1 (janvier 2004), 65–98.

[CPP08] CAZALS F., PARAMESWARAN A., PION S.: Robust Construction of the Three-Dimensional Flow Complex. In *ACM Symposium on Computational Geometry (SCG)* (Washington, United States, juin 2008).

[CSEH05] COHEN-STEINER D., EDELSBRUNNER H., HARER J.: Stability of persistence diagrams. In *Proceedings of the Twenty-First Annual Symposium on Computational Geometry* (New York, NY, USA, 2005), SCG '05, Association for Computing Machinery, p. 263–271.

[DZ04] DEY T. K., ZHAO W.: Approximate medial axis as a Voronoi subcomplex. *Computer-Aided Design. Vol. 36*, Num. 2 (2004), 195–202. Solid Modeling and Applications.

[EH08] EDELSBRUNNER H., HARER J.: Persistent homology—a survey. *Discrete and Computational Geometry - DCG. Vol. 453* (01 2008).

[GLBMR16] GONZALEZ-LORENZO A., BAC A., MARI J.-L., REAL P.: Two Measures for the Homology Groups of Binary Volumes. In *19th IAPR International Conference on Discrete Geometry for Computer Imagery (DGCI 2016)* (Nantes, France, avril 2016), Springer, (Ed.), vol. 9647 de *Discrete Geometry for Computer Imagery*, pp. 154–165.

[GRB11] GIESEN J., RAMOS E., BARDIA S.: Medial axis approximation and unstable flow complex. *International Journal of Computational Geometry and Applications. Vol. 18* (11 2011).

[Hat] HATCHER A.: *Algebraic Topology*.

[Lie03] LIEUTIER A.: Any open bounded subset of $\mathbb{R}^n$ has the same homotopy type than its medial axis. p. 65.

[OPT*15] OTTER N., PORTER M., TILLMANN U., GRINDROD P., HARRINGTON H.: A roadmap for the computation of persistent homology. *EPJ Data Science. Vol. 6* (06 2015).

[Sie96] SIERSMA D.: Voronoi diagrams and Morse theory of the distance function.

[SMM20] SUNDAR B., MUKUNDAN M., MUTHUGANAPATHY R.: A unified approach towards computing Voronoi diagram, medial axis, Delaunay graph and α-hull of planar closed curves using touching discs. *Computers and Graphics. Vol. 89* (05 2020).

[TDS*16] TAGLIASACCHI A., DELAME T., SPAGNUOLO M., AMENTA N., TELEA A.: 3d skeletons: A state-of-the-art report. *Computer Graphics Forum. Vol. 35* (05 2016).

[ZJH07] ZHOU Q.-Y., JU T., HU S.: Topology repair of solid models using skeletons. *IEEE Transactions on Visualization and Computer Graphics. Vol. 13* (2007).

Appendix

We want to prove the theorem 3.1 :

Theorem. *Given X an open bounded set of $\mathbb{R}^n$ and $t \geq 0$:*

$$\mathcal{F}_{-t}\left(\check{\mathcal{M}}(X)\right) = \check{\mathcal{M}}\left(\mathcal{F}_{-t}(X)\right)$$

Let $t > 0$ (case $t = 0$ is trivial).

Firstly, let's prove the two following lemmas:

Lemma 5.0.1.

$$\partial\mathcal{F}_{-t}(X) \subset sdf^{-1}(\{-t\})$$

Proof of lemma 5.0.1. $t > 0$ so $\mathcal{F}_{-t}(X) = sdf^{-1}(]-\infty,-t[)$ and is open because sdf is continue.
Moreover the complementary of $sdf^{-1}(]-\infty,-t[)$ in $\mathbb{R}^n$ is $sdf^{-1}([-t,+\infty[)$.
By definition, the boundary of an open T is $\partial T = \overline{T} \cap T^c$, where $\overline{T}$ is the closure of T and T^c its complementary. Hence, the boundary of $\mathcal{F}_{-t}(X)$ is:

$$\partial\mathcal{F}_{-t}(X) = \overline{sdf^{-1}(]-\infty,-t[)} \cap sdf^{-1}([-t,+\infty[)$$

By continuity of sdf, the sdf value of a point in $\overline{sdf^{-1}(]-\infty,-t[)}$ is in $]-\infty,-t]$.
Therefore, the sdf value of a point in $\partial\mathcal{F}_{-t}(X)$ is in $]-\infty,-t] \cap [-t,+\infty[= \{-t\}$. □

Lemma 5.0.2.

$$\forall c \in \mathcal{F}_{-t}(X), \quad d(c,\partial X) = d(c,\partial\mathcal{F}_{-t}(X)) + t$$

Proof of lemma 5.0.2. Let's take c in $\mathcal{F}_{-t}(X)$.

- We choose $s \in A_{\mathcal{F}_{-t}(X)}(c)$ and $\hat{s} \in A_X(s)$. We have the following inequality by triangular inequality:

$$\begin{aligned} d(c,\partial X) &\le d(c,\hat{s}) \\ &\le d(c,s) + d(s,\hat{s}) \\ &\le d(c,\mathcal{F}_{-t}(X)) + d(s,\partial X) \end{aligned}$$

  By using the definition of $A_{\mathcal{F}_{-t}(X)}(c)$ and $A_X(s)$.
  $s \in \partial\mathcal{F}_{-t}(X)$ so $d(s,\partial X) = t$ by lemma 5.0.1. This implies:

$$d(c,\partial X) \le d(c,\mathcal{F}_{-t}(X)) + t \tag{2}$$

- Conversely, by contradiction, suppose

$$d(c,\partial X) < d(c,\partial\mathcal{F}_{-t}(X)) + t \tag{3}$$

  Then let $\hat{s} \in A_X(c)$. As $d(c,\partial X) \ge t > 0$, we define:

$$\begin{aligned} \lambda &= \frac{d(c,\partial X) - d(c,\partial\mathcal{F}_{-t}(X)) + t}{2d(c,\partial X)} \\ s &= \lambda c + (1-\lambda)\hat{s} \end{aligned}$$

  Thus, we have:

$$d(c,s) = (1-\lambda)d(c,\hat{s}) = \frac{d(c,\partial X) + d(c,\partial\mathcal{F}_{-t}(X)) - t}{2}$$

$$d(c,s) < d(c,\partial\mathcal{F}_{-t}(X)) \qquad \text{using 3.}$$

  So, as c is in $\mathcal{F}_{-t}(X)$, we have $s \in \mathcal{F}_{-t}(X)$.
  Moreover we have:

$$d(s,\hat{s}) = \lambda\, d(c,\hat{s}) = \frac{d(c,\partial X) - d(c,\partial\mathcal{F}_{-t}(X)) + t}{2}$$

$$d(s,\hat{s}) < t \qquad \text{using 3.}$$

  So $d(s,\partial X) \le d(s,\hat{s}) < t$, therefore we have $s \notin \mathcal{F}_{-t}(X)$.
  By contradiction we have $d(c,\partial X) \ge d(c,\partial\mathcal{F}_{-t}(X)) + t$.

Thus, with 2 we get:

$$d(c,\partial X) = d(c,\partial\mathcal{F}_{-t}(X)) + t$$

□

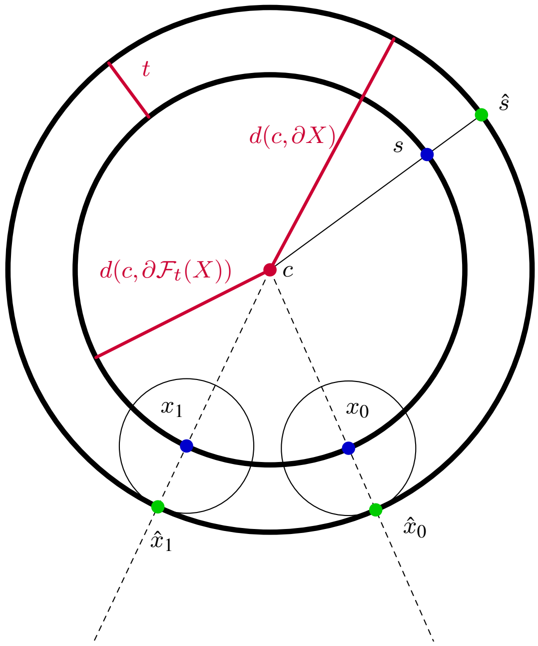

Figure 8: Scheme of the different points defined in the proof of the theorem 3.1 and lemma 5.0.2.

Proof of theorem 3.1.

- **Proof of** $\mathcal{F}_{-t}\Big(\check{\mathcal{M}}(X)\Big) \subset \check{\mathcal{M}}\Big(\mathcal{F}_{-t}(X)\Big)$:
  let $c \in \mathcal{F}_{-t}\Big(\check{\mathcal{M}}(X)\Big)$. We have directly $c \in \check{\mathcal{M}}(X)$ so we choose $\hat{x}_0, \hat{x}_1 \in A_X(c)$ such that $\hat{x}_0 \ne \hat{x}_1$.
  As $d(c,\partial X) \ge t > 0$, we define:

$$\begin{aligned} \mu &= \frac{t}{d(c,\partial X)} \\ x_0 &= \mu c + (1-\mu)\hat{x}_0 \\ x_1 &= \mu c + (1-\mu)\hat{x}_1 \end{aligned}$$

  We easily have $x_0 \ne x_1$, now let's show that they belong to $A_{\mathcal{F}_{-t}(X)}(c)$ in order to prove that $c \in \check{\mathcal{M}}\Big(\mathcal{F}_{-t}(X)\Big)$.
  Let $i \in \{0,1\}$. Let's prove that $x_i \in \partial\mathcal{F}_{-t}(X)$. We have:

$$\begin{aligned} d(x_i,c) &= (1-\mu)d(c,\hat{x}_i) \\ &= d(c,\partial X) - t \end{aligned}$$

  So by lemma 5.0.2: $d(x_i,c) = d(c,\partial\mathcal{F}_{-t}(X))$.

We build the following sequence:

$$x_i^k = \frac{1}{k}c + \left(1 - \frac{1}{k}\right)x_i$$

$(x_i^k)_{k\in\mathbb{N}}$ converges to x_i and stays in $\mathcal{F}_{-t}(X)$ as $d(c, x_i^k) = (1-1/n)d(c, x_i) < d(c, \partial\mathcal{F}_{-t}(X))$. Therefore, $x_i \in \overline{\mathcal{F}_{-t}(X)}$.
Moreover, we have:

$$\begin{aligned} d(x_i, \hat{x}_i) &= \mu\, d(c, \hat{x}_i) \\ &= t \end{aligned}$$

So, as $\hat{x}_i \in \partial X$, $d(x_i, \partial X) \leq t$.
This implies $x_i \notin \mathcal{F}_{-t}(X)$. x_i is in the closure of $\mathcal{F}_{-t}(X)$ but not in it, therefore it belongs to $\partial\mathcal{F}_{-t}(X)$.

As we have $x_i \in \partial\mathcal{F}_{-t}(X)$ and $d(c, \partial\mathcal{F}_{-t}(X)) = d(c, x_i)$ we have $x_i \in A_{\mathcal{F}_{-t}(X)}(c)$.
This conclude the fact that $c \in \check{\mathcal{M}}\Big(\mathcal{F}_{-t}(X)\Big)$.

- **Proof of** $\check{\mathcal{M}}\Big(\mathcal{F}_{-t}(X)\Big) \subset \mathcal{F}_{-t}\Big(\check{\mathcal{M}}(X)\Big)$:
let $c \in \check{\mathcal{M}}\Big(\mathcal{F}_{-t}(X)\Big)$. We choose $x_0, x_1 \in A_{\mathcal{F}_{-t}(X)}(c)$ such that $x_0 \neq x_1$.

Let $i \in \{0,1\}$. Let $\hat{x}_i \in A_X(x_i)$. $x_i \in \partial\mathcal{F}_{-t}(X)$ so by lemma 5.0.1 we have $d(\hat{x}_i, x_i) = t$. By triangular inequality we have:

$$\begin{aligned} d(\hat{x}_i, c) &\leq d(\hat{x}_i, x_i) + d(x_i, c) \\ &\leq t + d(c, \partial\mathcal{F}_{-t}(X)) \\ &\leq d(c, \partial X) \qquad \text{by lemma 5.0.2} \end{aligned} \tag{4}$$

And by minimality $d(c, \partial X) \leq d(\hat{x}_i, c)$.
As a result: $d(c, \partial X) = d(\hat{x}_i, c)$ so $\hat{x}_i$ belongs to $A_X(c)$ (because $\hat{x_i}$ is in ∂X as it is in $A_X(x_i)$).

In addition, we are in the equal case of the triangular inequality 4, which means that $\hat{x}_i$, x_i and c are co-linear.
As $d(c, \partial X) > 0$, we get:

$$\begin{aligned} x_0 &= \mu c + (1-\mu)\hat{x}_0 \\ x_1 &= \mu c + (1-\mu)\hat{x}_1 \\ &(\text{with } \mu = \frac{t}{d(c, \partial X)}) \end{aligned}$$

Hence we easily have $\hat{x}_0 \neq \hat{x}_1$ since $x_0 \neq x_1$. Therefore $|A_X(c)| > 1$ so c belongs to $\check{\mathcal{M}}(X)$ and $sdf^{-1}(]-\infty, -t[)$.
This conclude the fact that $c \in \mathcal{F}_{-t}\Big(\check{\mathcal{M}}(X)\Big)$.

$\square$